Metabolome analysis of esophageal cancer tissues using capillary electrophoresis-time-of-flight mass spectrometry

MASANORI TOKUNAGA[1,2], KENJIRO KAMI[3], SOJI OZAWA[2], JUNYA OGUMA[2], AKIHITO KAZUNO[2], HAYATO MIYACHI[4], YOSHIAKI OHASHI[3], MASATOSHI KUSUHARA[5] and MASANORI TERASHIMA[1]

[1]Division of Gastric Surgery, Shizuoka Cancer Center, Shizuoka 411-8777; [2]Department of Gastroenterological Surgery, Tokai University School Medicine, Isehara, Kanagawa 259-1193; [3]Human Metabolome Technologies, Inc., Tsuruoka, Yamagata 997-0052; [4]Department of Laboratory Medicine, Tokai University School Medicine, Isehara, Kanagawa 259-1193; [5]Regional Resources Division, Shizuoka Cancer Center, Shizuoka 411-8777, Japan

Received December 12, 2017; Accepted March 15, 2018

DOI: 10.3892/ijo.2018.4340

Abstract. Reports of the metabolomic characteristics of esophageal cancer are limited. In the present study, we thus conducted metabolome analysis of paired tumor tissues (Ts) and non-tumor esophageal tissues (NTs) using capillary electrophoresis time-of-flight mass spectrometry (CE-TOFMS). The Ts and surrounding NTs were surgically excised pairwise from 35 patients with esophageal cancer. Following tissue homogenization and metabolite extraction, a total of 110 compounds were absolutely quantified by CE-TOFMS. We compared the concentrations of the metabolites between Ts and NTs, between pT1 or pT2 (pT1-2) and pT3 or pT4 (pT3-4) stage, and between node-negative (pN^-) and node-positive (pN^+) samples. Principal component analysis and hierarchical clustering analysis revealed clear metabolomic differences between Ts and NTs. Lactate and citrate levels in Ts were significantly higher (P=0.001) and lower (P<0.001), respectively, than those in NTs, which corroborated with the Warburg effect in Ts. The concentrations of most amino acids apart from glutamine were higher in Ts than in NTs, presumably due to hyperactive glutaminolysis in Ts. The concentrations of malic acid (P=0.015) and citric acid (P=0.008) were significantly lower in pT3-4 than in pT1-2, suggesting the downregulation of tricarboxylic acid (TCA) cycle activity in pT3-4. On the whole, in this study, we demonstrate significantly different metabolomic characteristics between tumor and non-tumor tissues and identified a novel set of metabolites that were strongly associated with the degree of tumor progression. A further understanding of cancer metabolomics may enable the selection of more appropriate treatment strategies, thereby contributing to individualized medicine.

Correspondence to: Professor Soji Ozawa, Department of Gastroenterological Surgery, Tokai University School Medicine, 143 Shimokasuya, Isehara, Kanagawa 259-1193, Japan
E-mail: sozawa@tokai.ac.jp

Key words: esophageal cancer, mass spectrometry, metabolome, Warburg effect, tumor progression

Introduction

Esophageal cancer is the eighth most common type of cancer and the sixth leading cause of cancer-related mortality worldwide. It is frequently observed in East Asia (1). The clinicopathological characteristics of esophageal cancer have been investigated and clarified. Pathological tumor depth, nodal status and stage are known to be strongly associated with the survival outcome, which has been recently improved with advancements in multimodal treatments (2). However, the long-term survival outcome remains dismal, and the 5-year survival rate of patients with potentially curable advanced esophageal cancer has been reported to be only 34-55%, according to recent randomized controlled trials (3,4). To improve this poor survival outcome, appropriate treatment strategies tailored for each individual patient are warranted. To achieve this, the biological characteristics and causal factors of the survival outcome require clarification. Recently, it has been reported that the progression of the disease may affect the biological activity of some metabolites (5,6).

Metabolome analysis may enable us to understand tumor-specific metabolic characteristics, which would facilitate the discovery of novel anticancer drug targets and therapeutic strategies (7). Thus far, comparative metabolomic profiling has been conducted for several cancer types, such as gastric, lung, prostate, or colorectal cancers (7,8). Metabolomic profiles of esophageal cancer have also been investigated using blood samples (5,9-12) or paired tumor and non-tumor tissues (5,13,14). Metabolomic analysis using blood is preferable for the identification of tumor markers by comprehensive analysis; however, it does not reflect the microenvironment of the tumor, which can only be clarified using tissue samples. In addition, the majority of previous studies have used either nuclear magnetic resonance (NMR) (13,14) or gas chromatography-mass spectrometry (GC-MS) (15) for analysis. However, capillary electrophoresis-mass spectrometry (CE-MS), which is specialized for the analysis of ionic metabolites and thus may lead to the identification of novel metabolic properties of

cancer, has rarely been used for the metabolomic analysis of paired tumor and non-tumor tissues. Furthermore, the associations between metabolomic characteristics and advancement of the disease or survival outcome have rarely been investigated and remain unclear. Although Wang *et al* clarified the associations between metabolomic characteristics and tumor stages, only 45 metabolites were identified by NMR analysis, and the associations between metabolomic characteristics and other clinical factors were not investigated (14).

Therefore, the aim of the present study was to clarify the potential association between pathological disease status and metabolome profiles of tissues in patients with esophageal cancer. We also investigated the differences in metabolomic characteristics between tumor and non-tumor tissues from patients with esophageal cancer.

Patients and methods

Patient characteristics. The present study was designed as a single-center, prospective observational study. The institutional review board of Tokai University (Isehara, Japan) approved the study protocol, which had the following inclusion criteria: i) Patients with histologically confirmed adenocarcinoma or squamous cell carcinoma of the esophagus undergoing curative esophagectomy; ii) the size of the primary tumor large enough to obtain 1 g of tumor tissue without affecting the pathological examination; iii) an age of 20 years or older; and iv) written informed consent. Pathological tumor depth, nodal status and stage were assigned according to the Japanese Classification of Esophageal Cancer, 11th edition (16).

Between May, 2012 and October, 2013, a total of 35 patients were enrolled in the present study, and 35 pairs of tumor (Ts) and non-tumor (NTs) esophageal tissues were obtained. The characteristics and pathological findings of the patients are presented in Table I. Neoadjuvant chemotherapy was administered to 17 patients, and the majority of patients underwent subtotal esophagectomy. The surgery was curative (R0) in 24 patients, and resulted in microscopic residual disease (R1) in 7 patients and macroscopic residual disease (R2) in 4 patients. The disease was advanced in the majority of the patients, and the pathological stage was III or IVa in 77% of the patients.

Tissue sampling and metabolite extraction. Tumor and surrounding tissues were surgically resected from each of the 35 patients with esophageal cancer immediately following esophagectomy. The resected tissue samples were promptly frozen in liquid nitrogen and stored at -80˚C until metabolite extraction. To inactivate enzymes, ~50 mg of frozen tissue was immersed into 1,500 μl of 50% acetonitrile/Milli-Q water containing internal standards [H3304-1002; Human Metabolome Technologies (HMT), Tsuruoka, Japan] at 0˚C. The tissue was homogenized 3 times at 1,500 rpm for 120 sec using a tissue homogenizer (Microsmash MS100R; Tomy Digital Biology Co., Ltd., Tokyo, Japan) before the homogenate was centrifuged at 2,300 x g and 4˚C for 5 min. Subsequently, 800 μl of the the upper aqueous layer were centrifugally filtered through a Millipore 5,000-Da cut-off filter at 9,100 x g and 4˚C for 120 min to remove proteins. The filtrate was centrifugally concentrated and re-suspended in 50 μl of Milli-Q water for

Table I. Characteristics of patients with adenocarcinoma or squamous cell carcinoma (SCC) of the esophagus.

Sex, n	
Male	30
Female	5
Age, years	
Median	67
Range	42-81
Performance status, n	
0	30
1	5
Neoajuvant chemotherapy, n	
+	17
-	18
Histology	
Well differientated SCC	13
Moderately differientated SCC	18
Poorly differientated SCC	4
Tumor diameter (mm)	
Median	55
Range	25-93
Lymphatic invasion	
-	6
+	29
Vascular invasion	
-	4
+	31
Tumor depth	
T1	1
T2	7
T3	23
T4	4
Nodal status	
N0	8
N1	5
N2	16
N3	5
N4	1
Number of lymph node metastases	
Median	2
Range	0-9
Stage	
I	0
II	8
III	22
IVa	5
Curability	
R0	24
R1	7
R2	4

capillary electrophoresis time-of-flight mass spectrometry (CE-TOFMS) analysis.

Metabolome analysis. Metabolome analysis was conducted by the Basic Scan package from HMT using CE-TOFMS based on previously described methods (17,18). Briefly, CE-TOFMS analysis was conducted using an Agilent CE capillary electrophoresis system equipped with an Agilent 6210 time-of-flight mass spectrometer (Agilent Technologies, Waldbronn, Germany). The systems were controlled by Agilent G2201AA ChemStation software version B.03.01 for CE (Agilent Technologies). The spectrometer was scanned from 50 to 1,000 *m/z*, and peaks were extracted using MasterHands automatic integration software (Keio University, Tsuruoka, Yamagata, Japan) to obtain peak information including *m/z*, peak area, and migration time (MT) (19). Signal peaks corresponding to isotopomers, adduct ions and other product ions of known metabolites were excluded, and based on their *m/z* values with the MTs, remaining peaks were annotated according to the HMT's proprietary metabolite database. The areas of the annotated peaks were normalized based on internal standard levels and sample quantities to obtain relative levels of each metabolite.

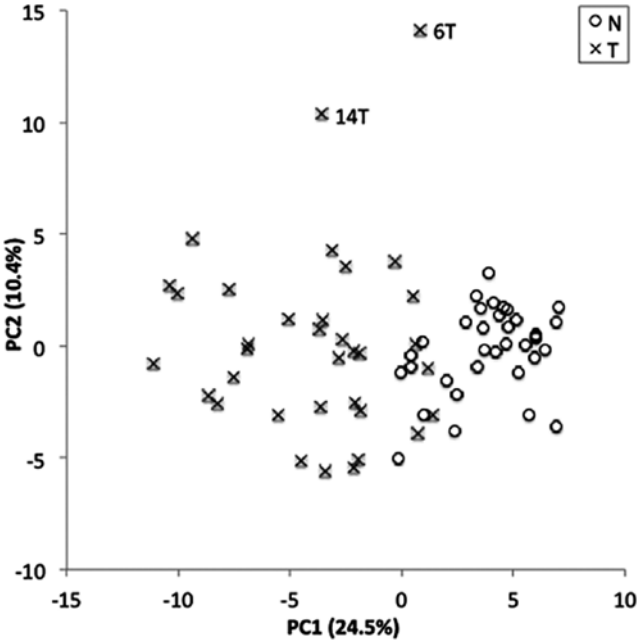

Figure 1. Principal component analysis plot.

Statistical analysis. Hierarchical cluster analysis (HCA) and principal component analysis (PCA) were performed using the proprietary software from HMT, PeakStat and SampleStat, respectively. Detected metabolites were plotted on metabolic pathway maps using VANTED software (20). All continuous data, including age, tumor diameter and the number of lymph node metastases, are presented as medians (range) and were analyzed by the Wilcoxon rank-sum test. A value of $P<0.05$ was considered to indicate a statistically significant difference. For any compound that was not detected in a tissue from the subjects, half of the minimum value of the measured compound replaced the missing data. Metabolomic profiles were compared between i) tumor and non-tumor tissues to elucidate differences in metabolomic profiles between them; ii) patients with T1 or T2 disease (pT1-2) and those with T3 or T4 disease (pT3-4); and iii) patients with node-negative (pN^-) and node-positive (pN^+) disease.

Results

Metabolomic characteristics between Ts and NTs. The metabolome data were normalized based on their z-values and used for PCA and HCA. The PCA plot presented in Fig. 1 shows a clear separation between NTs and Ts along the PC1 axis, indicating an apparently different metabolomic profile between NTs and Ts. The PCA plot also indicates a higher heterogeneity in the metabolomic profiles of Ts than of NTs. According to the HCA presented in Fig. 2, approximately two thirds of all the measured metabolites were higher in Ts than in NTs.

Metabolites measured in the present analysis were visualized on a metabolome-wide pathway map (available upon requested), and Fig. 3 illustrates the pathway map of the tricarboxylic acid (TCA) cycle. A total of 110 compounds were measured, and 99 compounds were absolutely quantified in this study (Table II). Of these, the concentrations of as many as 58 compounds were statistically significantly different between Ts and NTs ($P<0.05$). Fig. 4 and Table II illustrate all the measured metabolites in this study listed in descending order and based on Ts/NTs ratios. The concentrations of most amino acids apart from glutamine were significantly higher in Ts than in NTs (Fig. 5). In addition, as shown in Table II, the levels of nucleoside triphosphates [adenosine triphosphate (ATP), cytidine triphosphate (CTP), guanosine-5'-triphosphate (GTP) and uridine-5'-triphosphate (UTP)] were statistically significantly lower in Ts, whereas those of nucleoside monophosphates, such as guanosine monophosphate (GMP) were much higher. The concentrations of isocitric acid, *cis*-aconitic acid and citric acid, which are the upstream TCA cycle intermediates, were significantly lower in Ts than in NTs, while the lactic acid level was significantly higher in Ts.

Metabolomics with pathological tumor depth (pT) and pathological nodal status (pN) relevance. Tumor depth is known to be associated with the expression levels of glucose transporter (21) and several glycolytic enzymes, such as hexokinase 2 (22) and pyruvate kinase M2 (23). Thus, in this study, the tumor concentrations of the quantified metabolites were compared between pT1-2 and pT3-4 tumor tissues. Table III presents a list of metabolites of which the concentrations were at least 1.5-fold higher (7 metabolites) or lower (21 metabolites) in pT3-4 than in pT1-2). The concentrations of glycolytic and pentose phosphate pathway intermediates were higher overall in subjects with advanced disease (pT3-4), and the ratios of glucose 1-phosphate, ribose 5-phosphate and ribulose 5-phosphate were 1.92, 1.58 and 1.56, respectively, and >1.5-fold higher in pT3-4 than pT1-2. By contrast, the concentrations of malic acid and citric acid, also TCA cycle intermediates, and most nucleotides were significantly lower in pT3-4 than in pT1-2, possibly rationalizing relatively hypoxic microenvironment of advanced tumor tissues (24). Moreover, adenine-, cytidine- and uridine-nucleotide concentrations were lower in pT3-4 than in pT1-2 tumors, while the glutathione and

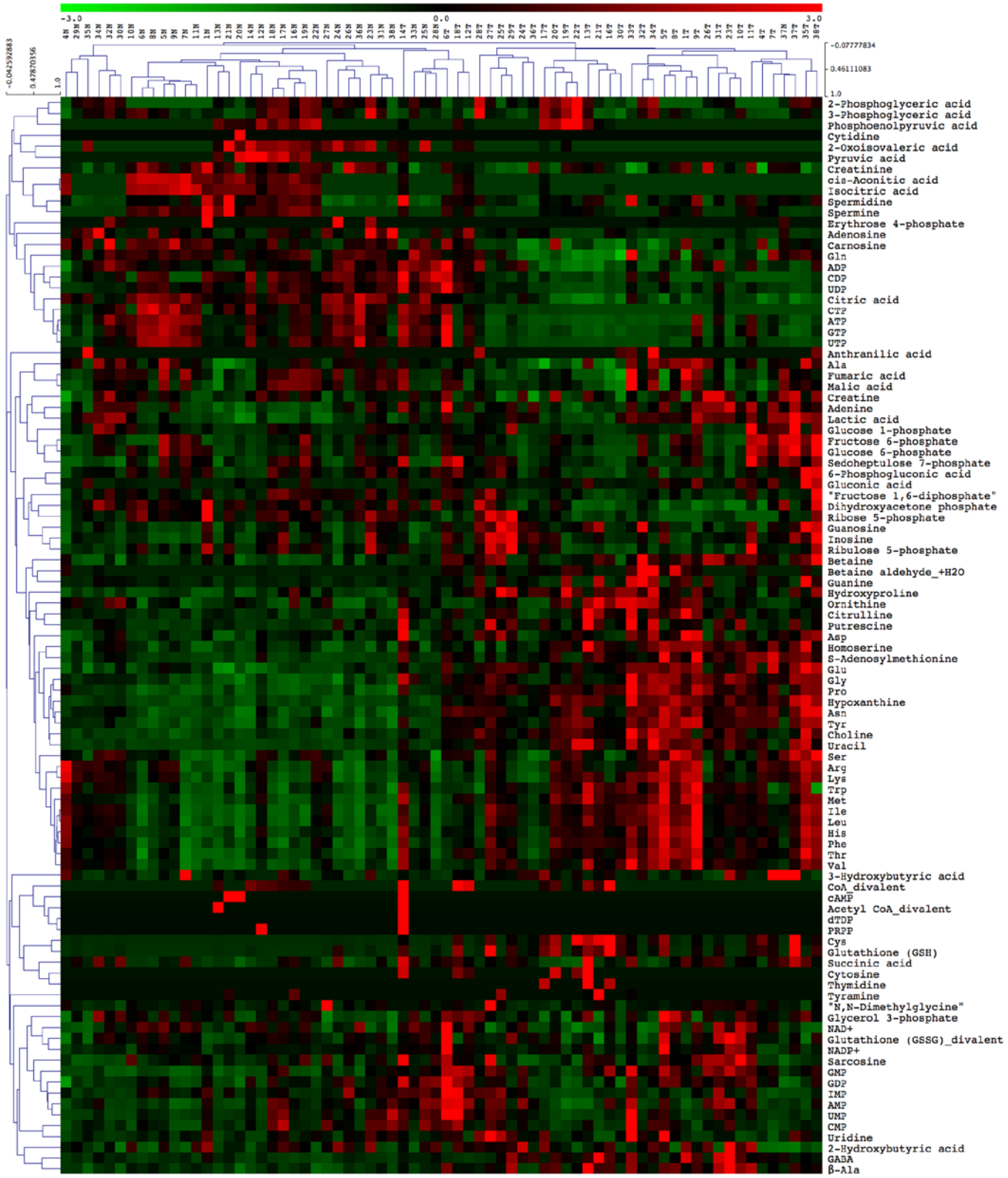

Figure 2. Heatmap of hierarchical cluster analysis.

cysteine levels were higher in pT3-4 than in pT1-2, with ratios being 1.80 and 3.36, respectively (Table III).

Metastatic alterations seemingly affect the balance of energy metabolism between glycolysis and oxidative phosphorylation (25,26). Jin *et al* identified a series of serum metabolites, such as valine and GABA that differ significantly in patients with esophageal squamous cell carcinoma with or without lymph node metastasis using a metabolomics approach (27). In this study, we thus investigated whether there was any metabolic difference in primary tumor tissues with or without metastasis. Table IV lists the metabolites the concentrations of which were at least 1.5-fold higher

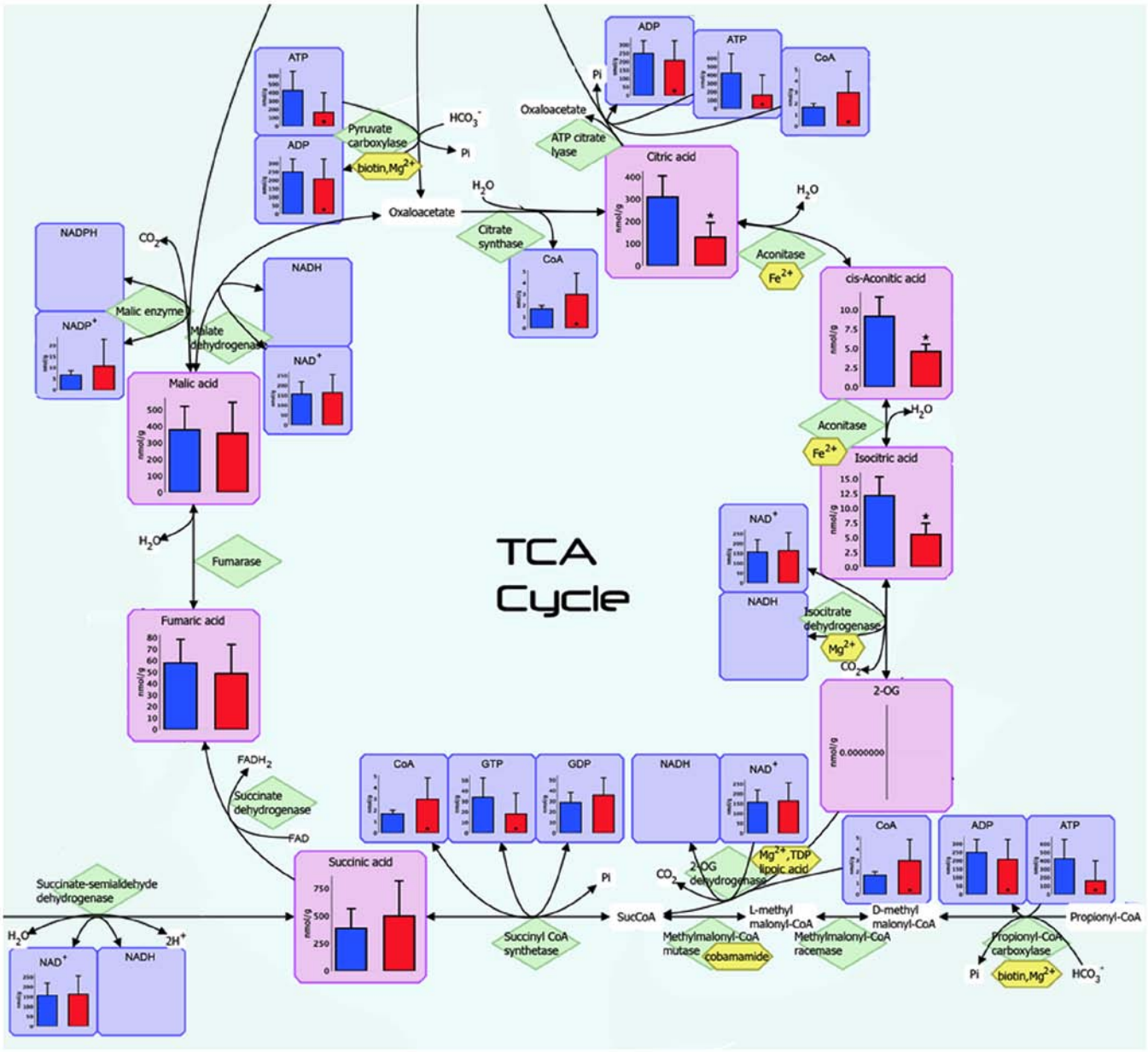

Figure 3. Metabolic pathway map comparing metabolite concentrations of tumor and non-tumor tissues. Blue bars indicate the concentration of non-tumor tissue, and red bars indicate that of tumor tissue.

(2 metabolites) or lower (18 metabolites) in pN^+ than in pN^-. *N,N*-dimethylglycine, isocitric acid, fructose 1,6-diphosphate and aspartic acid were statistically significantly lower in the pN^+ than the pN^- tumor tissues. Of note, many nucleotide concentrations including ATP, GTP, CTP and UTP tended to be lower in the pN^+ than pN^- tumors, although the difference was not statistically significant, with the exception of IMP and UMP.

Discussion

Thus far, metabolomic differences between tumor and non-tumor tissues have been investigated elsewhere in various types of cancer (7,8,13,14). The results of the present study not only demonstrated the basal metabolomic differences between esophageal tumor and non-tumor tissues, but also identified intriguing associations of metabolites with the degree of tumor advancement and with the presence or absence of lymph node metastasis.

Statistical significances between Ts and NTs were found in 58 out of 110 compounds, including isocitric acid, *cis*-aconitic acid, and citric acid, which were significantly lower in Ts than NTs, and lactic acid, which was significantly higher in Ts. These features suggest the upregulation of glycolysis and lactate formation, and the downregulation of the flux into the TCA cycle, and thus corroborate the hallmark of cancer metabolism i.e., the Warburg effect (7,28).

In the present study, the tumor concentrations of all amino acids apart from glutamine were higher than their non-tumor counterparts. Amino acid synthesis may be globally enhanced; however, this does not explain the significantly higher concentrations of even essential amino acids. The data thus possibly imply the hyperactivity of amino acid transporters (29-31) or autophagic protein degradation (32), both of which contribute

Table II. Concentrations of compounds (listed in descending order based on Ts/NTs ratios) in Ts and NTs.

Name of compound	NTs	Ts	Ratio (Ts/NTs)	P-value	ND/all (70)	ND/NTs (35)	ND/Ts (35)
2-Oxoglutaric acid	0.000	0.000	NA	NA	70	35	35
cGMP	0.000	0.000	NA	NA	70	35	35
dATP	0.000	0.000	NA	NA	70	35	35
dCTP	0.000	0.000	NA	NA	70	35	35
dTMP	0.000	0.000	NA	NA	70	35	35
dTTP	0.000	0.000	NA	NA	70	35	35
Glyceraldehyde 3-phosphate	0.000	0.000	NA	NA	70	35	35
Glycolic acid	0.000	0.000	NA	NA	70	35	35
Glyoxylic acid	0.000	0.000	NA	NA	70	35	35
Malonyl CoA_divalent	0.000	0.000	NA	NA	70	35	35
Thymine	0.000	0.000	NA	NA	70	35	35
Cys	2.737	182.622	66.72	<0.001	19	16	3
Glutathione (GSH)	55.380	839.397	15.16	<0.001	13	10	3
Uracil	21.761	168.667	7.75	<0.001	1	1	0
Betaine aldehyde_+H_2O	0.094	0.674	7.20	<0.001	45	31	14
Hypoxanthine	170.444	746.527	4.38	<0.001	0	0	0
S-Adenosylmethionine	12.254	40.406	3.30	<0.001	0	0	0
Putrescine	36.506	119.342	3.27	<0.001	0	0	0
Gluconic acid	28.168	87.567	3.11	<0.001	0	0	0
Guanine	15.205	43.218	2.84	0.226	2	0	2
GMP	29.556	76.026	2.57	<0.001	0	0	0
Met	97.882	243.854	2.49	<0.001	0	0	0
GABA	12.250	30.295	2.47	<0.001	0	0	0
Tyramine	0.166	0.408	2.46	0.404	64	33	31
Choline	161.699	395.925	2.45	<0.001	0	0	0
Homoserine	0.843	2.001	2.37	<0.001	12	10	2
Pro	377.514	890.493	2.36	<0.001	0	0	0
Citrulline	30.403	69.160	2.27	<0.001	0	0	0
Asn	124.410	275.376	2.21	<0.001	0	0	0
Tyr	140.516	307.546	2.19	<0.001	0	0	0
Hydroxyproline	28.391	58.942	2.08	<0.001	0	0	0
β-Ala	36.973	75.260	2.04	<0.001	0	0	0
Betaine	47.056	94.012	2.00	<0.001	0	0	0
Ile	265.350	510.584	1.92	<0.001	0	0	0
Leu	492.049	914.861	1.86	<0.001	0	0	0
Phe	229.967	418.200	1.82	<0.001	0	0	0
Asp	403.697	729.062	1.81	<0.001	0	0	0
Guanosine	16.504	28.872	1.75	0.001	0	0	0
Gly	1615.687	2817.176	1.74	<0.001	0	0	0
Glu	1862.762	3242.047	1.74	<0.001	0	0	0
CoA_divalent	0.575	0.984	1.71	0.463	54	28	26
His	222.272	375.296	1.69	<0.001	0	0	0
Val	564.942	937.011	1.66	<0.001	0	0	0
$NADP^+$	6.226	10.256	1.65	0.142	5	3	2
Inosine	118.058	193.143	1.64	<0.001	0	0	0
Adenine	0.945	1.510	1.60	<0.001	0	0	0
Thr	540.238	841.303	1.56	<0.001	0	0	0
Trp	56.496	87.291	1.55	<0.001	0	0	0
Cytosine	0.075	0.113	1.50	0.011	64	35	29
Ornithine	102.318	150.059	1.47	0.010	0	0	0
Uridine	50.310	72.303	1.44	0.108	0	0	0
AMP	234.908	327.723	1.40	0.170	0	0	0

Table II. Continued.

Name of compound	NTs	Ts	Ratio (Ts/NTs)	P-value	ND/all (70)	ND/NTs (35)	ND/Ts (35)
Sarcosine	11.929	16.584	1.39	0.091	0	0	0
Fructose 6-phosphate	13.418	18.209	1.36	0.196	7	5	2
Lactic acid	30047.277	40727.323	1.36	0.001	0	0	0
UMP	39.626	53.320	1.35	0.320	0	0	0
Lys	728.484	958.409	1.32	0.002	0	0	0
Succinic acid	385.179	497.439	1.29	0.140	0	0	0
Arg	396.418	507.514	1.28	0.010	0	0	0
GDP	28.004	35.686	1.27	0.036	1	1	0
Glycerol 3-phosphate	211.332	268.640	1.27	0.054	0	0	0
Sedoheptulose 7-phosphate	19.238	24.436	1.27	0.095	0	0	0
Ser	467.826	590.577	1.26	0.077	0	0	0
3-Hydroxybutyric acid	287.678	355.980	1.24	0.051	0	0	0
Glucose 1-phosphate	25.489	31.150	1.22	0.362	0	0	0
IMP	31.863	37.742	1.18	0.506	1	0	1
Glutathione (GSSG)_divalent	560.285	663.095	1.18	0.674	0	0	0
Glucose 6-phosphate	84.783	99.749	1.18	0.870	0	0	0
Thymidine	1.100	1.273	1.16	0.082	67	35	32
CMP	10.600	12.012	1.13	0.664	7	5	2
2-Hydroxybutyric acid	115.702	130.960	1.13	0.344	0	0	0
Ribulose 5-phosphate	33.894	37.243	1.10	0.753	0	0	0
Spermidine	17.565	18.966	1.08	0.326	0	0	0
Creatine	1608.615	1719.858	1.07	0.907	0	0	0
Anthranilic acid	0.233	0.249	1.07	0.241	63	33	30
6-Phosphogluconic acid	15.030	15.899	1.06	0.318	3	1	2
2-Phosphoglyceric acid	8.473	8.918	1.05	0.812	21	10	11
N,*N*-Dimethylglycine	3.640	3.802	1.04	0.398	3	1	2
PRPP	1.423	1.486	1.04	1.000	68	34	34
NAD^+	156.517	163.076	1.04	0.815	0	0	0
dTDP	0.656	0.675	1.03	0.331	69	35	34
Phosphoenolpyruvic acid	4.217	4.285	1.02	0.947	50	25	25
Ala	1740.699	1756.570	1.01	0.788	0	0	0
Acetyl CoA_divalent	0.411	0.414	1.01	1.000	68	34	34
cAMP	0.425	0.422	0.99	0.592	67	33	34
Fructose 1,6-diphosphate	66.853	66.265	0.99	0.072	1	1	0
Cytidine	3.452	3.356	0.97	0.331	69	34	35
Malic acid	377.443	357.165	0.95	0.362	0	0	0
3-Phosphoglyceric acid	74.824	69.761	0.93	0.247	0	0	0
Creatinine	57.646	51.442	0.89	0.051	0	0	0
ADP	248.784	207.315	0.83	0.011	0	0	0
Fumaric acid	57.785	47.315	0.82	0.019	1	0	1
Gln	2277.779	1703.272	0.75	<0.001	0	0	0
Ribose 5-phosphate	11.736	7.814	0.67	<0.001	11	1	10
UDP	42.200	27.604	0.65	<0.001	0	0	0
Carnosine	2.419	1.397	0.58	<0.001	4	0	4
Dihydroxyacetone phosphate	28.798	16.384	0.57	<0.001	5	0	5
Pyruvic acid	24.610	13.810	0.56	0.011	61	27	34
GTP	34.037	17.962	0.53	<0.001	0	0	0
CDP	7.051	3.378	0.48	<0.001	14	6	8
Spermine	10.261	4.708	0.46	0.151	19	10	9
Citric acid	308.711	128.575	0.42	<0.001	0	0	0
Adenosine	8.060	3.157	0.39	<0.001	0	0	0
ATP	424.260	162.969	0.38	<0.001	0	0	0

Table II. Continued.

Name of compound	NTs	Ts	Ratio (Ts/NTs)	P-value	ND/all (70)	ND/NTs (35)	ND/Ts (35)
Erythrose 4-phosphate	5.064	1.801	0.36	0.042	63	29	34
cis-Aconitic acid	5.724	2.025	0.35	<0.001	47	16	31
UTP	77.543	24.624	0.32	<0.001	3	0	3
Isocitric acid	7.347	2.204	0.30	<0.001	46	16	30
2-Oxoisovaleric acid	5.466	1.498	0.27	<0.001	47	17	30
CTP	14.088	2.946	0.21	<0.001	28	4	24

ND, not detected; cGMP, cyclic guanosine monophosphate; dATP, deoxyadenosine triphosphate; dCTP, deoxycytidine 5'-triphosphate; dTMP, deoxythymidine monophosphate; dTTP, deoxythymidine triphosphate; Cys, cysteine; GMP, guanosine monophosphate; GABA, gamma-aminobutyric acid; Pro, proline; Asn, asparagine; Tyr, tyrosine; β-Ala, β-alanine; Ile, isoleucine; Leu, leucine; Phe, phenylalanine; Asp, aspartic acid; Gly, glycine; Glu, glutamic acid; His, histidine; Val, valine; NADP, nicotinamide adenine dinucleotide phosphate; Thr, threonine; Trp, tryptophan; AMP, adenosine monophosphate; UMP, uridine monophosphate; Lys, lysine; Arg, arginine; GDP, guanosine diphosphate; Ser, serine; IMP, inosine monophosphate; CMP, cytidine monophosphate; PRPP, phosphoribosyl diphosphate; NAD, nicotinamide adenine dinucleotide; dTDP, deoxythymidine diphosphate; Ala, alanine; cAMP, cyclic adenosine monophosphate; ADP, adenosine diphosphate; Gln, glutamine; UDP, uridine diphosphate; GTP, guanosine triphosphate; CDP, cytidine diphosphate; ATP, adenosine triphosphate; UTP, uridine triphosphate; CTP, cytidine triphosphate.

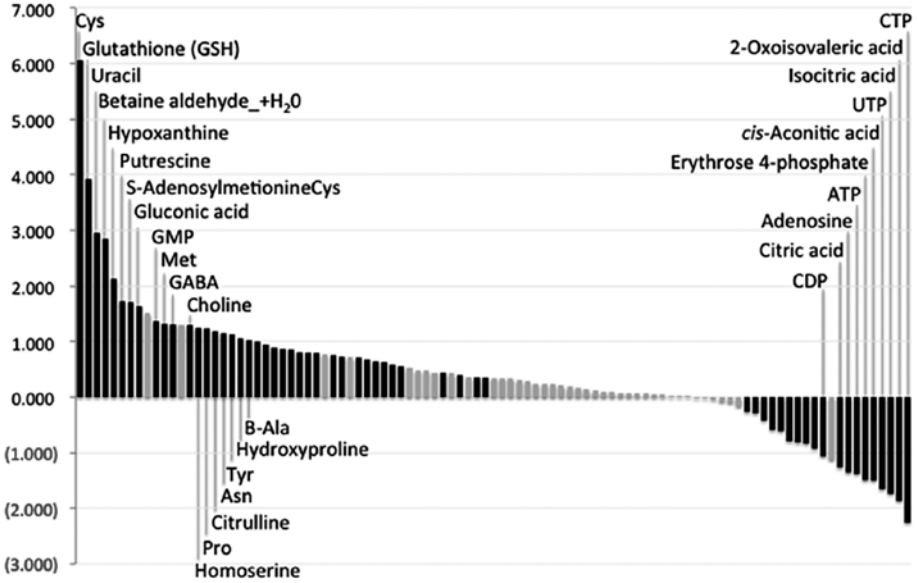

Figure 4. Log_2 [tumor tissue (Ts)/non-tumor esophageal tissues (NTs)] of metabolites shown in descending order. Metabolites with statistical significance are shown in black. Among these, the names of metabolites are provided when the Ts/NTs ratios were >2.0 or <0.05.

to the accumulation of overall amino acids in tumor tissues. Glutamine, however, was the only amino acid that was lower in the tumor than the non-tumor tissues. This is presumably due to hyperactive glutamine breakdown, or glutaminolysis, for producing energy and building blocks for continuous proliferation (33,34). In fact, this trend of overall accumulations of amino acids apart from glutamine in tumor regions has been reported elsewhere (7,8,14); accordingly, the near universality of this tumor amino acid profile is intriguing, and the result is reported herein for the first time (at least to the best of our knowledge) for an esophageal tumor.

Few studies have investigated the association between metabolomic characteristics and the pathological status of tumor tissues. However, Wang *et al* reported 12 key metabolites, such as glucose, AMP, NAD, formate, creatine and choline metabolites that exhibited strong associations with the advancement of esophageal cancer, and are thus likely to be involved in both the carcinogenic process and metastatic alteration of esophageal cancer (14). While attempting to corroborate previous studies, we identified a novel set of metabolites that show significant correlations with the advancement of cancer, such as glycolytic and pentose phosphate pathway intermediates (Table III), taking advantage of CE-TOFMS-based metabolomics, which is best suited to ionic metabolite analysis.

In contrast to glycolytic and pentose phosphate pathway intermediates, the concentrations of citric acid, isocitric acid and malic acid in pT3-4 disease were relatively lower than in pT1-2 disease, suggesting the downregulation of TCA cycle activity in advanced tumors. These results, i.e., a lower TCA

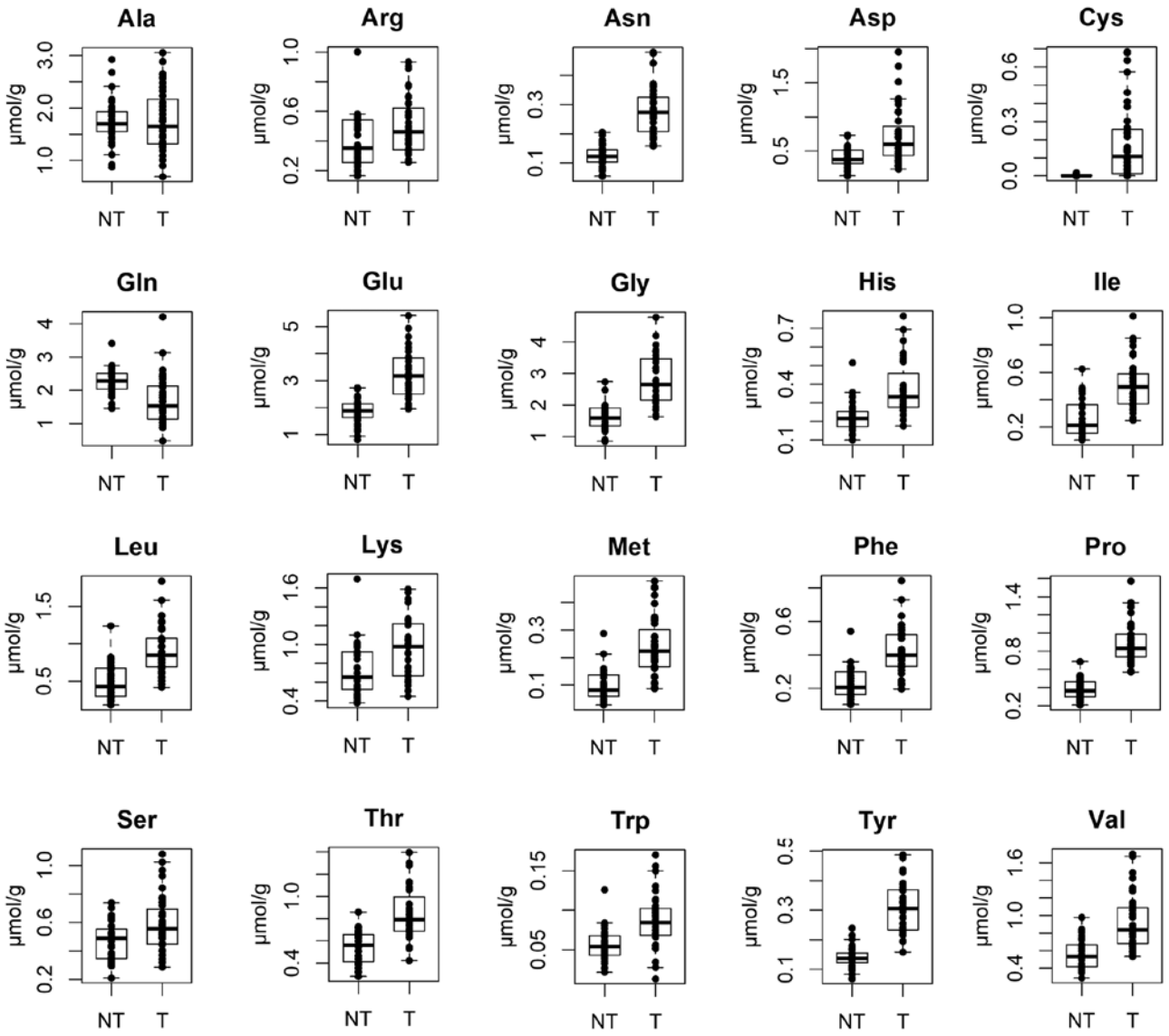

Figure 5. Concentrations of amino acids between tumor tissue (Ts) and non-tumor esophageal tissues (NTs). Ala, alanine; Arg, arginine; Asn, asparagine; Asp, aspartic acid; Cys, cysteine; Gln, glutamine; Glu, glutamic acid; Gly, glycine; His, histidine; Ile, isoleucine; Leu, leucine; Lys, lysine; Met, methionine; Phe, phenylalanine; Pro, proline; Ser, serine; Thr, threonine; Trp, tryptophan; Tyr, tyrosine; Val, valine.

cycle activity and accelerated glycolysis, may be due to a more enhanced Warburg effect in advanced-stage tumors compared with less advanced ones.

A series of nucleotide concentrations were lower in advanced than in less advanced tumors (Table III). Although higher levels of nucleotide metabolites in the advanced tumors were expected, the nucleotide pathway intermediates were mostly lower in the advanced ones. This is possibly due to accelerated utilizations of these nucleotides for their increased DNA synthesis. A lower adenosine monophosphate level in advanced than in less advanced tumors has also been previously reported (14). Total adenylate levels (ATP + ADP + AMP) in pT3-4 (579.8 nmol/g tissue) was almost half of those in pT1-2 (1096.8 nmol/g), again indicating a higher demand of nucleotides in pT3-4 than in pT1-2 tumor tissues for their increased DNA synthesis. The levels of glutathione and cysteine, two primary anti-oxidants, were on average higher in pT3-4 than in pT1-2, indicating a more reduced status and higher resistance against oxidative stress in pT3-4.

Of note, in cases with pN^+, both glutathione and cysteine levels were lower than in cases with pN^-, with ratios being 0.50 (P=0.130) (Table IV) and 0.83, respectively, translating to a lower resistance against oxidative stress in pN^+ (note that the ratio of cysteine is not shown in Table IV). Generally, the tumor microenvironment is in a highly oxidative state, and thus, tumor cells tend to be more resistant to oxidative stress. Pavlides *et al* (35) proposed that stromal tissues rely primarily on glycolysis, producing lactate and ketones, whereas metastatic cancer cells rather use oxidative phosphorylation for energy production, availing the carbon sources provided by the neighboring stromal tissues, and coined the term, 'reverse Warburg effect' (35,36). In this perspective, proliferative tumor regions may contain more cells that mainly use typical Warburg-type energy metabolism, which presumably reduces oxidative stress assuming that oxidative phosphorylation via electron transport chain is a primary source of reactive oxygen species (ROS) (37). By contrast, metastatic tumor cells are rich in mitochondria, producing higher concentrations of ROS,

Table III. Concentrations of compounds in pT1-2 and pT3-4, and the pT3-4/pT1-2 ratio.

Compound name	pT1-2	pT3-4	Ratio (pT3-4/pT1-2)	P-value
CTP	7.968	1.459	0.18	0.022
UTP	60.532	13.984	0.23	0.651
UDP	63.988	16.823	0.26	0.088
CDP	7.582	2.133	0.28	0.030
UMP	110.416	36.403	0.33	0.010
IMP	76.817	26.164	0.34	0.046
CMP	23.980	8.466	0.35	0.007
ATP	290.826	125.085	0.43	0.406
GTP	29.731	14.475	0.49	0.143
2-Oxoisovaleric acid	2.399	1.231	0.51	0.033
AMP	517.276	271.559	0.52	0.019
CoA_divalent	1.549	0.817	0.53	0.818
$NADP^+$	15.262	8.773	0.57	0.112
GDP	51.221	31.083	0.61	0.009
Citric acid	182.291	112.659	0.62	0.008
Spermidine	26.808	16.642	0.62	0.104
Malic acid	502.515	314.098	0.63	0.015
NAD^+	228.540	143.680	0.63	0.034
ADP	288.720	183.195	0.63	0.104
Sarcosine	22.653	14.786	0.65	0.017
Isocitric acid	2.992	1.971	0.66	0.287
Ribulose 5-phosphate	26.049	40.560	1.56	0.143
Ribose 5-phosphate	5.390	8.532	1.58	0.858
Guanosine	18.390	31.977	1.74	0.042
Glutathione (GSH)	520.187	933.978	1.80	0.356
Glucose 1-phosphate	18.228	34.979	1.92	0.923
Tyramine	0.146	0.486	3.33	0.972
Cys	64.742	217.549	3.36	0.103

CTP, cytidine triphosphate; UTP, uridine triphosphate; UDP, uridine diphosphate; CDP, cytidine diphosphate; UMP, uridine monophosphate; IMP, inosine monophosphate; CMP, cytidine monophosphate; ATP, adenosine triphosphate; GTP, guanosine triphosphate; AMP, adenosine monophosphate; NADP, nicotinamide adenine dinucleotide phosphate; GDP, guanosine diphosphate; NAD, nicotinamide adenine dinucleotide; ADP, adenosine diphosphate; Cys, cysteine.

Table IV. Concentrations of compounds in pN^- and pN^+, and the pN^+/pN^- ratio.

Compound name	N^-	N^+	Ratio (N^+/N^-)	P-value
CoA_divalent	2.094	0.656	0.31	0.201
N,*N*-Dimethylglycine	6.492	3.004	0.46	0.010
ATP	268.010	131.845	0.49	0.630
Glutathione (GSH)	1361.444	684.717	0.50	0.130
IMP	58.624	31.555	0.54	0.027
UTP	37.779	20.726	0.55	0.280
CDP	5.071	2.877	0.57	0.374
Sedoheptulose 7-phosphate	36.054	20.993	0.58	0.061
UMP	78.125	45.970	0.59	0.019
Ribulose 5-phosphate	54.332	32.180	0.59	0.286
Isocitric acid	3.199	1.909	0.60	0.039
GTP	25.892	15.612	0.60	0.428
Fructose 1,6-diphosphate	94.459	57.911	0.61	0.015
Asp	1030.898	639.629	0.62	0.041
CTP	4.155	2.588	0.62	0.830
UDP	38.597	24.347	0.63	0.056
Ribose 5-phosphate	10.923	6.893	0.63	0.538
2-Oxoisovaleric acid	2.042	1.337	0.65	0.287
Guanine	30.862	46.879	1.52	0.860
Phosphoenolpyruvic acid	2.537	4.803	1.89	0.825

ATP, adenosine triphosphate; IMP, inosine monophosphate; UTP, uridine triphosphate; CDP, cytidine diphosphate; UMP, uridine monophosphate; GTP, guanosine triphosphate; Asp, aspartic acid; GTP, guanosine triphosphate; UDP, uridine diphosphate.

and thus may develop a tumor microenvironment with higher oxidative stress (25,26,36). Taken together, the results thus reflect the basal metabolic differences between advanced (but without metastatic) and metastatic tumors.

The present study is limited to the elucidation of the metabolic microenvironment of tissues with or without cancerous cells and may not be suitable for discovery of a potential biomarker for early detection of cancer, as our analysis was performed using surgically resected specimens and not liquid biopsies. Although not as comprehensive as our study, the metabolomics of biopsy specimens are being realized (38-40). Moreover, once we focus on some specific metabolite markers for pathological tumor status and survival outcome, a minimal amount of tissue, such as a biopsy specimen, may be sufficient for such targeted analysis.

A limitation of this study is that the effects of potential confounding factors affecting the metabolome characteristics, such as the use of chemotherapy and each patient's nutritional status, could not be eliminated. Therefore, the difference in metabolome characteristics between advanced and less-advanced tumors might have been influenced by these confounding factors. Due to the limited number of cases in this study, it would be difficult to exclude the effects of all potential confounding factors completely; however, these effects should be clarified in future trials with sufficient numbers of cases.

In conclusion, in this study, we demonstrated significantly different metabolomic characteristics between tumor and non-tumor tissues of esophageal cancer and identified a novel

set of metabolites that correlate well with the degree of tumor advancement. This suggests that the pathological disease status and survival outcome may be predicted by analysis of several primary metabolites, possibly even from a biopsy specimen. Further clarification of cancer metabolomics, particularly in relation to the advancement of disease and survival outcome, will enable the selection of more appropriate treatment strategies contributing to individualized medicine.

Acknowledgements

The authors would like to thank Dr Tamaki Fujimori and Ms. Aya Hoshi, HMT, for their data analysis support. The authors used the English Language Service (International Medical Information Center) for language editing.

Funding

This study was supported by the Japan Society for the Promotion of Science (JSPS) KAKENHI (Grant no. JP26461998).

Availability of data and materials

The analyzed datasets generated during the study are available from the corresponding author on reasonable request.

Ethics approval and consent to participate

The Institutional Review Board of Tokai University (Isehara, Japan) approved the study protocol and all patients provided written informed consent prior to obtaining the samples.

Authors' contributions

MTo, KK and SO conceived and designed the study; MTo, KK, JO and AK were involved in data acquisition; KK and YO were involved in data analysis; MTo, KK, SO, HM, MK and MTe were involved in data interpretation. All authors have read and approval the final manuscript.

Consent for publication

Not applicable.

Competing interests

The authors declare that they have no competing interests.

References

1. Domper Arnal MJ, Ferrández Arenas Á and Lanas Arbeloa Á: Esophageal cancer: Risk factors, screening and endoscopic treatment in Western and Eastern countries. World J Gastroenterol 21: 7933-7943, 2015.
2. Tachimori Y, Ozawa S, Numasaki H, Fujishiro M, Matsubara H, Oyama T, Shinoda M, Toh Y, Udagawa H and Uno T: Comprehensive Registry of Esophageal Cancer in Japan, 2008. Esophagus 12: 130-157, 2015.
3. van Hagen P, Hulshof MC, van Lanschot JJ, Steyerberg EW, van Berge Henegouwen MI, Wijnhoven BP, Richel DJ, Nieuwenhuijzen GA, Hospers GA, Bonenkamp JJ, *et al*; CROSS Group: Preoperative chemoradiotherapy for esophageal or junctional cancer. N Engl J Med 366: 2074-2084, 2012.
4. Ando N, Kato H, Igaki H, Shinoda M, Ozawa S, Shimizu H, Nakamura T, Yabusaki H, Aoyama N, Kurita A, *et al*: A randomized trial comparing postoperative adjuvant chemotherapy with cisplatin and 5-fluorouracil versus preoperative chemotherapy for localized advanced squamous cell carcinoma of the thoracic esophagus (JCOG9907). Ann Surg Oncol 19: 68-74, 2012.
5. Abbassi-Ghadi N, Kumar S, Huang J, Goldin R, Takats Z and Hanna GB: Metabolomic profiling of oesophago-gastric cancer: A systematic review. Eur J Cancer 49: 3625-3637, 2013.
6. Pavlova NN and Thompson CB: The emerging hallmarks of cancer metabolism. Cell Metab 23: 27-47, 2016.
7. Kami K, Fujimori T, Sato H, Sato M, Yamamoto H, Ohashi Y, Sugiyama N, Ishihama Y, Onozuka H, Ochiai A, *et al*: Metabolomic profiling of lung and prostate tumor tissues by capillary electrophoresis time-of-flight mass spectrometry. Metabolomics 9: 444-453, 2013.
8. Hirayama A, Kami K, Sugimoto M, Sugawara M, Toki N, Onozuka H, Kinoshita T, Saito N, Ochiai A, Tomita M, *et al*: Quantitative metabolome profiling of colon and stomach cancer microenvironment by capillary electrophoresis time-of-flight mass spectrometry. Cancer Res 69: 4918-4925, 2009.
9. Ikeda A, Nishiumi S, Shinohara M, Yoshie T, Hatano N, Okuno T, Bamba T, Fukusaki E, Takenawa T, Azuma T, *et al*: Serum metabolomics as a novel diagnostic approach for gastrointestinal cancer. Biomed Chromatogr 26: 548-558, 2012.
10. Xu J, Chen Y, Zhang R, Song Y, Cao J, Bi N, Wang J, He J, Bai J, Dong L, *et al*: Global and targeted metabolomics of esophageal squamous cell carcinoma discovers potential diagnostic and therapeutic biomarkers. Mol Cell Proteomics 12: 1306-1318, 2013.
11. Zhang X, Xu L, Shen J, Cao B, Cheng T, Zhao T, Liu X and Zhang H: Metabolic signatures of esophageal cancer: NMR-based metabolomics and UHPLC-based focused metabolomics of blood serum. Biochim Biophys Acta 1832: 1207-1216, 2013.
12. Ma H, Hasim A, Mamtimin B, Kong B, Zhang HP and Sheyhidin I: Plasma free amino acid profiling of esophageal cancer using high-performance liquid chromatography spectroscopy. World J Gastroenterol 20: 8653-8659, 2014.
13. Yang Y, Wang L, Wang S, Liang S, Chen A, Tang H, Chen L and Deng F: Study of metabonomic profiles of human esophageal carcinoma by use of high-resolution magic-angle spinning 1H NMR spectroscopy and multivariate data analysis. Anal Bioanal Chem 405: 3381-3389, 2013.
14. Wang L, Chen J, Chen L, Deng P, Bu Q, Xiang P, Li M, Lu W, Xu Y, Lin H, *et al*: 1H-NMR based metabonomic profiling of human esophageal cancer tissue. Mol Cancer 12: 25, 2013.
15. Wu H, Xue R, Lu C, Deng C, Liu T, Zeng H, Wang Q and Shen X: Metabolomic study for diagnostic model of oesophageal cancer using gas chromatography/mass spectrometry. J Chromatogr B Analyt Technol Biomed Life Sci 877: 3111-3117, 2009.
16. The Japan Eshophageal Society: Japanese Classification of Esophageal Cancer 11th edition. Esophagus: Nov 10, 2016 (Epub ahead of print).
17. Ohashi Y, Hirayama A, Ishikawa T, Nakamura S, Shimizu K, Ueno Y, Tomita M and Soga T: Depiction of metabolome changes in histidine-starved Escherichia coli by CE-TOFMS. Mol Biosyst 4: 135-147, 2008.
18. Ooga T, Sato H, Nagashima A, Sasaki K, Tomita M, Soga T and Ohashi Y: Metabolomic anatomy of an animal model revealing homeostatic imbalances in dyslipidaemia. Mol Biosyst 7: 1217-1223, 2011.
19. Sugimoto M, Wong DT, Hirayama A, Soga T and Tomita M: Capillary electrophoresis mass spectrometry-based saliva metabolomics identified oral, breast and pancreatic cancer-specific profiles. Metabolomics 6: 78-95, 2010.
20. Junker BH, Klukas C and Schreiber F: VANTED: A system for advanced data analysis and visualization in the context of biological networks. BMC Bioinformatics 7: 109, 2006.
21. Kawamura T, Kusakabe T, Sugino T, Watanabe K, Fukuda T, Nashimoto A, Honma K and Suzuki T: Expression of glucose transporter-1 in human gastric carcinoma: Association with tumor aggressiveness, metastasis, and patient survival. Cancer 92: 634-641, 2001.
22. Hamabe A, Yamamoto H, Konno M, Uemura M, Nishimura J, Hata T, Takemasa I, Mizushima T, Nishida N, Kawamoto K, *et al*: Combined evaluation of hexokinase 2 and phosphorylated pyruvate dehydrogenase-E1α in invasive front lesions of colorectal tumors predicts cancer metabolism and patient prognosis. Cancer Sci 105: 1100-1108, 2014.

23. Fukuda S, Miyata H, Miyazaki Y, Makino T, Takahashi T, Kurokawa Y, Yamasaki M, Nakajima K, Takiguchi S, Mori M, *et al*: Pyruvate kinase M2 modulates esophageal squamous cell carcinoma chemotherapy response by regulating the pentose phosphate pathway. Ann Surg Oncol 22 (Suppl 3): S1461-S1468, 2015.
24. Hockel M, Schlenger K, Aral B, Mitze M, Schaffer U and Vaupel P: Association between tumor hypoxia and malignant progression in advanced cancer of the uterine cervix. Cancer Res 56: 4509-4515, 1996.
25. Payen VL, Porporato PE, Baselet B and Sonveaux P: Metabolic changes associated with tumor metastasis, part 1: Tumor pH, glycolysis and the pentose phosphate pathway. Cell Mol Life Sci 73: 1333-1348, 2016.
26. Porporato PE, Payen VL, Baselet B and Sonveaux P: Metabolic changes associated with tumor metastasis, part 2: Mitochondria, lipid and amino acid metabolism. Cell Mol Life Sci 73: 1349-1363, 2016.
27. Jin H, Qiao F, Chen L, Lu C, Xu L and Gao X: Serum metabolomic signatures of lymph node metastasis of esophageal squamous cell carcinoma. J Proteome Res 13: 4091-4103, 2014.
28. Warburg O: On the origin of cancer cells. Science 123: 309-314, 1956.
29. Honjo H, Kaira K, Miyazaki T, Yokobori T, Kanai Y, Nagamori S, Oyama T, Asao T and Kuwano H: Clinicopathological significance of LAT1 and ASCT2 in patients with surgically resected esophageal squamous cell carcinoma. J Surg Oncol 113: 381-389, 2016.
30. Kobayashi H, Ishii Y and Takayama T: Expression of L-type amino acid transporter 1 (LAT1) in esophageal carcinoma. J Surg Oncol 90: 233-238, 2005.
31. Younes M, Pathak M, Finnie D, Sifers RN, Liu Y and Schwartz MR: Expression of the neutral amino acids transporter ASCT1 in esophageal carcinomas. Anticancer Res 20: 3775-3779, 2000.
32. Morselli E, Galluzzi L, Kepp O, Vicencio JM, Criollo A, Maiuri MC and Kroemer G: Anti- and pro-tumor functions of autophagy. Biochim Biophys Acta 1793: 1524-1532, 2009.
33. Vander Heiden MG, Cantley LC and Thompson CB: Understanding the Warburg effect: The metabolic requirements of cell proliferation. Science 324: 1029-1033, 2009.
34. Tsun ZY and Possemato R: Amino acid management in cancer. Semin Cell Dev Biol 43: 22-32, 2015.
35. Pavlides S, Whitaker-Menezes D, Castello-Cros R, Flomenberg N, Witkiewicz AK, Frank PG, Casimiro MC, Wang C, Fortina P, Addya S, *et al*: The reverse Warburg effect: Aerobic glycolysis in cancer associated fibroblasts and the tumor stroma. Cell Cycle 8: 3984-4001, 2009.
36. Sotgia F, Whitaker-Menezes D, Martinez-Outschoorn UE, Flomenberg N, Birbe RC, Witkiewicz AK, Howell A, Philp NJ, Pestell RG and Lisanti MP: Mitochondrial metabolism in cancer metastasis: Visualizing tumor cell mitochondria and the 'reverse Warburg effect' in positive lymph node tissue. Cell Cycle 11: 1445-1454, 2012.
37. Orrenius S: Reactive oxygen species in mitochondria-mediated cell death. Drug Metab Rev 39: 443-455, 2007.
38. Benahmed MA, Elbayed K, Daubeuf F, Santelmo N, Frossard N and Namer IJ: NMR HRMAS spectroscopy of lung biopsy samples: Comparison study between human, pig, rat, and mouse metabolomics. Magn Reson Med 71: 35-43, 2014.
39. Li M, Song Y, Cho N, Chang JM, Koo HR, Yi A, Kim H, Park S and Moon WK: An HR-MAS MR metabolomics study on breast tissues obtained with core needle biopsy. PLoS One 6: e25563, 2011.
40. Choi JS, Baek HM, Kim S, Kim MJ, Youk JH, Moon HJ, Kim EK and Nam YK: Magnetic resonance metabolic profiling of breast cancer tissue obtained with core needle biopsy for predicting pathologic response to neoadjuvant chemotherapy. PLoS One 8: e83866, 2013.